Journal of Integrative Neuroscience

*J. Integr. Neurosci.* **2022**; 21(3): 75
https://doi.org/10.31083/j.jin2103075

*Original Research*

# Effects of sinoaortic denervation on hemodynamic perturbations of prolonged paradoxical sleep deprivation and rapid cold stress in rats

Yia-Ping Liu[1,2], Chen-Cheng Lin[2], Yu-Chieh Lin[3], Shih-Hung Tsai[4,*,†], Che-Se Tung[2,3,*,†]

[1]Department of Psychiatry, Cheng Hsin General Hospital, 11280 Taipei, Taiwan
[2]Department of Physiology, National Defense Medical Center, 11490 Taipei, Taiwan
[3]Division of Medical Research & Education, Cheng Hsin General Hospital, 11280 Taipei, Taiwan
[4]Department of Emergency Medicine, Tri-service General Hospital, National Defense Medical Center, 11490 Taipei, Taiwan
*Correspondence: ch83883739@gmail.com (Che-Se Tung); tsaishihung@yahoo.com.tw (Shih-Hung Tsai)
[†]These authors contributed equally.
Academic Editor: Luigi De Gennaro
Submitted: 11 November 2021 Revised: 20 December 2021 Accepted: 8 January 2022 Published: 6 April 2022

**Abstract**

**Background**: Sleep disturbances and aversive cold stress (CS) are cardiovascular risk factors. This study investigates how homeostatic control autonomic baroreflex influences the hemodynamic perturbations evoked by paradoxical sleep deprivation (PSD) and CS. **Methods**: Conscious adult male rats were randomly divided into four groups (Sham/CON [control], Sham/PSD, sinoaortic denervation [SAD]/CON, and SAD/PSD). Spectral analysis and SAD were employed to evaluate the effects of a 72-hr PSD with 10-min CS on blood pressure variability and heart rate variability (BPV and HRV) at total power (TP) and three frequency power densities, very-low-frequency (VLF), low frequency (LF), and high frequency (HF). **Results**: Key findings showed: (I) Compared with the control sham surgery (Sham/CON), in the natural baseline (PreCS) trial, SAD surgery (SAD/CON) causes high systolic blood pressure (SBP), heart rate (HR), increases LFBPV (low-frequency power of BPV), LF/HFHRV (the ratio LF/HF of HRV), and TPBPV (the total power of BPV), but decreases HFHRV (high-frequency power of HRV) and VLFHRV (very-low-frequency power of HRV) than the Sham/CON does. In the CS trial, SAD/CON increases the CS-induced pressor, increases the CS-elicited spectral density, LF/HFHRV, but decreases HFBPV than the Sham/CON does. (II) Compared with SAD/CON and Sham/PSD (PSD under sham surgery), in both PreCS and CS trials, SAD/PSD (PSD under SAD) causes high SBP and HR than both SAD/CON and Sham/PSD their SBP and HR. In PreCS, SAD-PSD also changes the spectral density, including increasing Sham-PSD's LFBPV, LF/HFHRV, VLFBPV, and TPBPV but decreasing Sham-PSD's VLFHRV and TPHRV. However, in CS, SAD-PSD changes the CS-elicited spectral density, including increasing Sham-PSD's VLFBPV, LF/HFHRV, and TPHRV but decreasing Sham-PSD's HFBPV and LFBPV. **Conclusion**: The results suggest baroreflex combined with other reflex pathways, such as inhibitory renorenal reflex, modulates the vascular and cardiorespiratory responses to PSD under PreCS and subsequent CS trials.

**Keywords:** Spectral analysis; Paradoxical sleep deprivation; Cold stress; Blood pressure variability; Heart rate variability; Sinoaortic denervation

## 1. Introduction

Arterial baroreflex is one of the most powerful and rapidly buffering mechanisms for short-term cardiovascular regulation in maintaining blood pressure (BP) and organ perfusion within a narrow range [1,2]. The most sensitive baroreceptors are in the carotid sinuses and aortic arch. Baroreceptor activity travels along afferent glossopharyngeal and vagus nerves directly into the central nervous system to activate efferent (outflow) parasympathetic nerve activity. Oppositely, it inhibits efferent sympathetic nerve activity to the heart and vasculature. Besides baroreflex, other reflex pathways involved in the homeostatic regulations are also familiar, such as cardiopulmonary, hepatic/portal, and renorenal reflexes [3–9].

Sleep disturbances and aversive cold stress (CS) are cardiovascular risk factors [10–12], highly prevalent, and often happen together. In the past, we have demonstrated that paradoxical sleep deprivation (PSD) rats in natural baseline (PreCS) result in sympathoexcitation and intensifying myogenic oscillations. However, in the aversive CS, PSD causes sympathoexcitation but weakens such myogenic changes [12]. We have also demonstrated that rapidly CS exposure produces pressor and tachycardia and increases sympathetic neurotransmissions, called cold-evoked hemodynamic perturbations (CEHP) [10], a non-invasive maneuver for clinical practice in evaluating autonomic cardiovascular regulation. CEHP phenomenon is characterized by hemodynamic instability (irregular BP, heart rate (HR), and cardiovascular myogenic oscillations), initial vasoconstriction followed by vasodilatation, and secondary progressive vasoconstriction.

Spectral analysis of blood pressure variability (BPV) and heart rate variability (HRV) using a frequency domain approach has been widely applied to evaluate the autonomic regulation of cardiovascular function in health and disease—a dynamic interplay among ongoing oscillatory BP and HR and compensatory responses, which depends

on a series of interactions among complex neuro-humoral reflexes [10,11,13–15].

Afferent baroreflex failure patients are often known due to carotid sinus nerve damage because of neck surgery or radiation [1]. Sinoaortic denervation (SAD) animal model has been used for baroreflex failure studies demonstrated by sympathoexcitation, increases BPV and BP, and increases efferent renal sympathetic nerve activity (ERSNA) and local angiotensin II levels [16–19]. On the other hand, the aforementioned renorenal reflex, also known as an inhibitory reflex, activates afferent renal nerve activity (ARNA), eliciting an ERSNA decrease that could prevent ERSNA overactivation and subsequent excessive sodium retention [4,20,21]. It has been reported that SAD animals are more reactive to environmental stimuli and exhibit exaggerated responses to cardiovascular challenges [1,22–25]. In the present study, we thus investigate autonomic baroreflex and spectral density changes using the SAD model rats to elucidate hemodynamic perturbations of PSD with and without the CS impact.

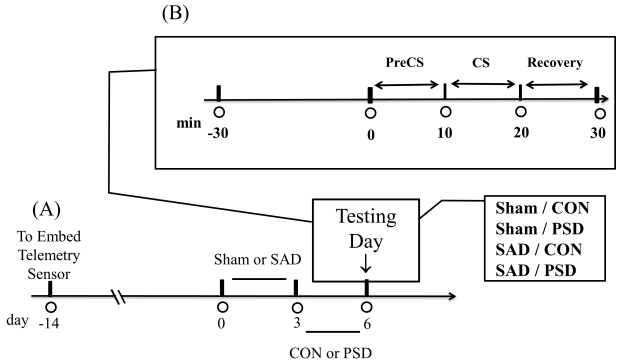


**Fig. 1. A general protocol.** (A) The telemetry sensor in rats 14 days before the sinoaortic denervation (SAD) or sham surgery. (B) After PSD (72-hr paradoxical sleep deprivation), the aversive cooling process started: PreCS, CS, and Recovery. The control group rats were subjected to sham surgery (Sham/CON). The other three group rats were subjected to Sham/PSD, SAD/CON, and SAD/PSD. Abbreviations: CS, cold stress; PreCS, before CS; CON, control.

## 2. Materials and methods

### *2.1 Ethical approval*

All the experiments were approved by the National Defense Medical Center (NDMC) animal care committee (IACUC-15-091). Experiments were carried out following the guidelines laid down by the animal ethics/welfare committee and conforming to the principles and regulations of this Journal.

### *2.2 Experimental procedure*

The experimental process of the present study is shown in Fig. 1. In brief, the SAD surgery was carried out 14 days following the telemetry sensor embedded. After three days of recovery, the rats experienced 72-hr PSD (see Fig. 1A), and then they were exposed to the aversive cooling process, during which their beat-to-beat SBP signals were recorded in the PreCS and the CS trials. The rat was then removed from the test cage, dried with a cloth, and placed in a similar cage for 10 min to facilitate recovery (see Fig. 1B).

### *2.3 Animals*

Forty-eight adult male Sprague-Dawley rats weighing between 300 and 350 g were received at the Laboratory Animal Center of NDMC one week before the experiments. Rats in the same experimental groups were housed together (3 rats/cage) in a temperature- and humidity-controlled holding facility with a 12-hr light/dark cycle (light on 07:00 to 19:00), given standard laboratory chow diet (Ralston Purina, St. Louis, MO, USA) and water ad libitum, and randomly subjected to 4 groups ($n$ = 12 for each): Sham/CON (control), Sham/PSD, SAD/CON, and SAD/PSD.

### *2.4 Telemetry sensor embed surgery*

Fourteen days before the SAD or sham surgery, a telemetry sensor (TL11M2-M2-C50-PXT, DSI, St. Paul, MN, USA) was implanted into the rat's abdominal cavity to record the core temperature. One catheter of this sensor was embedded in the ascending aorta to record BP and HR.

### *2.5 Sinoaortic denervation*

Rats were subjected to SAD or sham surgery with anesthesia by intraperitoneal 30 mg/kg sodium pentobarbital. SAD was performed according to that described by Krieger with minor modifications [26]. Briefly, a 3-cm midline incision was made and reflected sternocleidomastoid muscles laterally to expose the neurovascular sheath. The common carotid arteries, carotid bifurcations, and internal and external carotid arteries branches were stripped of all tissue attachments and then painted with 10% ethanol under a surgical microscope. After completing the operation, all rats will be placed in the recovery chamber and allowed three days to recover before the test session.

### *2.6 Paradoxical sleep deprivation*

The PSD method used for Sham/PSD or SAD/PSD group rats has been modified by us previously employed from Ferraz's water platform technique [12]. A container ($35 \times 18 \times 25$ cm$^3$) contains a circular platform (6.5 cm in diameter) for the PSD establishment. The water level was set up to 1 cm below the platform level and then acclimated the animal to the water environment with access to food and water ad libitum. This method takes advantage of a rat entering paradoxical sleep losing its postural control due to decreased muscle tone; thus, paradoxical sleep is interrupted.

### 2.7 Cooling process and signal recording

The test cage for the cooling process is identical to the container of rats used in the PSD. After adjusting to the experimental environments, all rats were taken to an adjacent room and treated with the same cooling process. A maximum of six rats was tested per day, with three rats tested simultaneously. All experiments were performed between 08:30 and 11:30.

Following a complete stabilization of the systolic BP (SBP) and HR at room temperature for 30 minutes, each rat's glabrous palms and soles were quickly submerged into ice water (4 °C) for the impact of cold stress (CS). Beat-to-beat SBP signals were recorded continuously at the subsequent trials: the 10-min before CS trial (PreCS) and the 10-min CS trial itself. After the CS trial, the rat was removed from the test cage. The results of signals from a 5-min period (minutes 3 to 8) were then adopted for spectral analyses in each trial.

### 2.8 Spectrum signal acquisition and processing

One hour before the experiment on the day of testing, the transmitter was magnetically activated. Pulse signals for calibration were generated as an analog signal (UA10; Data Sciences International, St. Paul, MN, USA) with a range of $\pm$5 V and a 12-bit resolution. Individual rats in each group were then placed on the top of the receivers (PhysioTel RPC-1) for telemetric signal acquisition. Five receivers were connected to a PC desktop computer via a matrix (Dataquest A.R.T. Data Exchange Matrix, Data Sciences International). The received signals were recorded with Dataquest acquisition software (Dataquest A.R.T. 4.33, KYS Technology Co., Ltd, New Taipei City, Taiwan). A series of successive SBP and inter-beat interval (IBI) signals measured throughout the experiments were then digitized at a 500 Hz sampling rate and processed offline using MATLAB software 2010 version (The MathWorks Inc., San Diego, CA, USA). The beat-by-beat oscillatory SBP and IBI signals were analyzed using autoregressive spectral decomposition to quantify their frequencies and spectral powers regarding BPV and HRV. The BPV calculation was based on software kindly written for us by P.L. Lee, National Central University, Taiwan. In brief, the acquired SBP signals were preprocessed by applying a band-pass filter (0.1–18 Hz, zero phases fourth-order) to remove the DC components. After identifying all the SBP peak maxima between 2 zero-cross points, the extracted beat-by-beat SBP time series were detrended, interpolated, and re-sampled at 0.05 s to generate a new time series of evenly spaced SBP samples, allowing direct spectral analysis of each distribution using a fast Fourier transform algorithm. The HRV calculation was based on Chart software developed by PowerLab (ADInstruments, Colorado Springs, CO, USA). For a 5 min period, we calculated the power densities of total power (0.00–3.0 Hz, TP), very low-frequency power (0.02–0.2 Hz, VLF), low-frequency power (0.20–0.60 Hz, LF), and high-frequency power (0.60–3.0 Hz, HF) [10]. The modulus of the spectral density for each frequency had units of BPV ($mmHg^2$) and HRV ($ms^2$). The power LF to HF (LF/HF ratio) as a measure of sympathovagal balance was also calculated. The squared coherence function was computed as the square of the cross-spectrum normalized by the product of the spectra of the BPV and HRV signals [27]. When the peak coherence value ($K^2_{IBI/SBP}$) exceeded 0.58 within a frequency range, these two signals were considered to covary significantly at that frequency.

### 2.9 Statistical analysis

Version 16.0 of the SPSS software (SPSS, Inc., Chicago, IL, USA) has been used to perform all statistics. The Kolmogorov–Smirnov normality test was performed for all data sets. Data were analyzed by multiple-way of analysis of variance (ANOVA) with between-subject factors of "sleep condition" (CON and PSD) and "surgical condition" (Sham and SAD). The cooling process data was further analyzed by within-subjects factor "trial" (PreCS and CS). For the intensity difference between PreCS and CS trials, two-way ANOVA was used, and "sleep condition" (CON and PSD) and "surgical condition" (Sham and SAD) were employed as the between-subjects factors. Data will split for the simple main effect if interactions have been found. *Post hoc* comparisons were carried out with the Tukey method. If it found no interactions of the main effect, planned comparisons were carried out with paired Student's *t*-test to interpret the data better. Data are presented as mean $\pm$ standard error (SEM). The difference was considered significant at $p < 0.05$.

## 3. Results

Fig. 1 displays the test session, a 30-min period for stabilization plus a 20-min period for the cooling process (PreCS and CS), conducted immediately after a 72-hr PSD regimen (i.e., six days after SAD surgery). Averaged data in both PreCS and CS trials are shown in Figs. 2,3,4,5, Table 1, and **Supplementary Tables 1,2,3** (see the Data Supplement).

### 3.1 The effects of PSD and SAD on SBP and HR throughout the experiment

For the changes of SBP and HR (Fig. 2 and **Supplementary Table 1**), multiple-way ANOVA revealed significant interactions among trial, sleep condition, and surgical condition (SBP and HR) and significant interactions between-subject factors: "trial and sleep condition (HR)", "trial and surgical condition (SBP and HR)", and "sleep condition and surgical condition (HR)". The differences between the two groups drove the significant interactions: Sham/CON and Sham/PSD ([PreCS]: HR; [CS]: SBP and HR), SAD/CON and SAD/PSD ([PreCS]: SBP and HR; [CS]: SBP and HR), Sham/CON and SAD/CON ([PreCS]:

**Table 1. The differences in systolic blood pressure (SBP) and heart rate (HR) levels and spectral power intensities between CS and PreCS trials in different group rats.**

| | Sham/CON | Sham/PSD | SAD/CON | SAD/PSD |
|---|---|---|---|---|
| SBP (△mmHg) | 19.00 ± 5.72 | 29.70 ± 6.42$^{a1}$ | 18.00 ± 7.38$^{b1}$ | 10.00 ± 4.63$^{b2}$ |
| VLF (△mmHg$^2$) | 2.12 ± 1.88 | 2.59 ± 1.79 | 1.41 ± 0.84 | 3.57 ± 1.78$^{c1}$ |
| LF (△mmHg$^2$) | 8.67 ± 2.42 | 17.56 ± 2.57$^{a3}$ | 6.21 ± 2.34$^{b3}$ | 5.65 ± 1.25$^{a1b3}$ |
| HF (△mmHg$^2$) | 14.91 ± 4.98 | 21.18 ± 1.76 | 4.18 ± 1.83$^{a3b3}$ | 2.90 ± 2.78$^{a3b2}$ |
| HR (△beats/min) | 110.43 ± 18.35 | 41.62 ± 15.41$^{a2}$ | 28.90 ± 13.76$^{a3}$ | 6.12 ± 14.99$^{a3}$ |
| VLF (△ms$^2$) | −9.32 ± 4.19 | −15.23 ± 5.22 | −0.12 ± 1.22$^{a3b3}$ | −1.16 ± 0.76$^{a3b2}$ |
| LF (△ms$^2$) | −0.81 ± 0.29 | −1.64 ± 0.08$^{a2}$ | −0.44 ± 0.38$^{b2}$ | −0.97 ± 0.32$^{b1}$ |
| HF (△ms$^2$) | −0.97 ± 1.79 | −3.87 ± 0.68$^{a1}$ | −1.16 ± 0.61$^{b3}$ | 0.57 ± 1.12$^{b2}$ |

Data are presented as mean ± standard error (SEM). Differences were assessed by two-way ANOVA followed by *post hoc* Tukey method or Planned comparisons with paired Student's *t*-test and are indicated as follows: $^a$compared with Sham/CON, $^b$compared with Sham/PSD, $^c$compared with SAD/CON. $^{1,2,3}p < 0.05$, 0.01, 0.001 respectably. Abbreviations: CS, cold stress; PreCS, before CS; CON, control; SAD, sinoaortic denervation; PSD, paradoxical sleep deprivation; VLF, very-low-frequency; LF, low frequency; HF, high frequency; BPV, blood pressure variability; HRV, heart rate variability; △, difference.

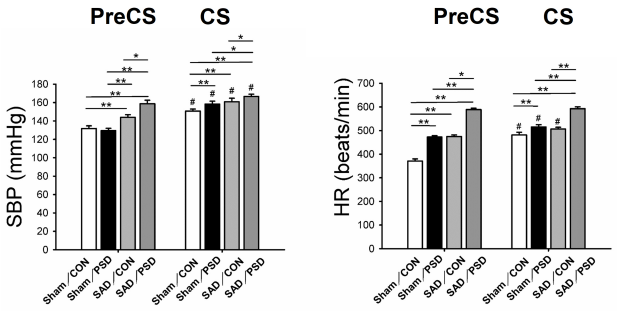


**Fig. 2. Effects on systolic blood pressure, SBP (A) and heart rate, HR (B) of different group rats throughout the experiment.** Data are presented as mean ± standard error (SEM). Differences were assessed by multiple-way ANOVA followed by *post hoc* Tukey method or Planned comparisons with paired Student's *t*-test and are indicated as follows: differences between group rats (*$p < 0.05$, **$p < 0.01$) and differences between the same parameter for CS versus PreCS (#$p < 0.05$). Abbreviations: CS, cold stress; PreCS, before CS.

SBP and HR; [CS]: SBP), and Sham/PSD and SAD/PSD ([PreCS]: SBP and HR; [CS]: SBP and HR). Further analysis by planned comparisons revealed significant differences between Sham/CON and SAD/PSD ([PreCS]: SBP and HR; [CS]: SBP and HR). The results indicate that SAD could augment the PSD's pressor and tachycardia responses in both PreCS and CS trials.

Multiple-way ANOVA also revealed a significant main effect of within-subjects factor "trial" (**Supplementary Table 1**) driven by the differences between PreCS and CS in four groups: Sham/CON (SBP and HR), Sham/PSD (SBP and HR), SAD/CON (SBP and HR), and SAD/PSD (SBP). For the intensity difference between PreCS and CS of SBP and HR (Table 1 and **Supplementary Table 2**), two-way ANOVA revealed significant main effects of SAD (SBP and HR) and PSD (HR), which were driven by the differences between two groups: Sham/CON and Sham/PSD (HR), Sham/CON and SAD/CON (HR), and Sham/PSD and SAD/PSD (SBP). Further analysis by planned comparisons revealed a significant difference between Sham/CON and SAD/PSD (HR) and Sham/PSD and SAD/CON (SBP). These results indicate that SAD/CON and SAD/PSD groups reduce the intensity difference between PreCS and CS in both SBP and HR of Sham/CON and Sham/PSD groups; this is because, in PreCS, the sympathoexcitatory pressor and tachycardia of SAD/CON or SAD/PSD groups are higher than pressor and tachycardia of Sham/CON or Sham/PSD groups.

### *3.2 The effects of PSD and SAD on spectral density throughout the experiment*

For the changes of spectral density (Fig. 3 and **Supplementary Table 3**), multiple-way ANOVA revealed significant interactions among trial, sleep condition, and surgical condition (LFBPV, HFBPV, and TPBPV) and significant interactions between-subject factors: "trial and sleep condition (LFBPV, LFHRV, HFBPV, and TPBPV)", "trial and surgical condition (VLFHRV, LFBPV, LFHRV, HFBPV, HFHRV, and TPBPV)", and "sleep condition and surgical condition (VLFBPV, LFBPV, LFHRV, HFBPV, and TPBPV)". The significant interactions were driven by the differences between two groups: Sham/CON and Sham/PSD ([PreCS]: LFBPV, LFHRV, HFBPV, HFHRV and TPBPV; [CS]: VLFHRV, LFBPV, HFBPV and TPHRV), SAD/CON and SAD/PSD ([PreCS]: VLFBPV, LFBPV, LFHRV and TPBPV; [CS]: VLFBPV, LFHRV and HFHRV), Sham/CON and SAD/CON ([PreCS]: VLFHRV, LFBPV, HFHRV, TPBPV, TPHRV and LF/HFHRV; [CS]: LFHRV, HFBPV, HFHRV and

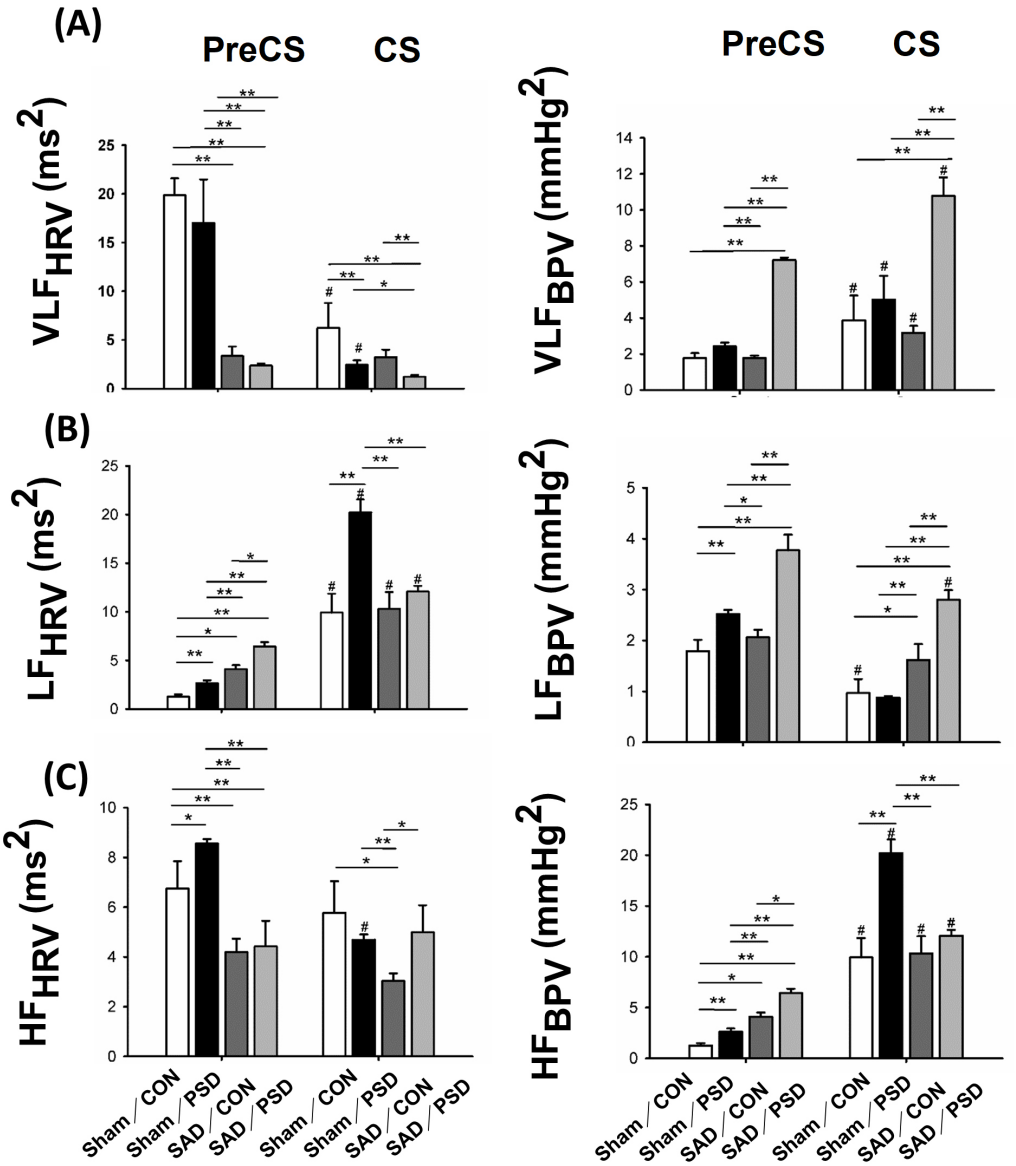


**Fig. 3. Effects on the mean spectral density of blood pressure variability (right panel) and heart rate variability (left panel) of different group rats throughout the experiment.** (A) the very-low-frequency power (VLF), (B) the low-frequency power (LF), and (C) the high-frequency power (HF). Data are presented as mean ± standard error (SEM). Differences were assessed by multiple-way ANOVA followed by post hoc Tukey method or Planned comparisons with paired Student's *t*-test and are indicated as follows: differences between group rats (*$p < 0.05$, **$p < 0.01$) and differences between the same parameter for CS versus PreCS (#$p < 0.05$). Abbreviations: CS, cold stress; PreCS, before CS; BPV, blood pressure variability; HRV, heart rate variability.

LF/HFHRV), and Sham/PSD and SAD/PSD ([PreCS]: VLFBPV, VLFHRV, LFBPV, LFHRV, HFBPV, TPBPV, TPHRV and LF/HFHRV; [CS]: VLFBPV, VLFHRV, LFBPV, LFHRV, HFBPV, TPHRV and LF/HFHRV). Further analysis by planned comparisons revealed a significant difference between Sham/CON and SAD/PSD ([PreCS]: VLFBPV, VLFHRV, LFBPV, LFHRV, HFHRV, TPBPV, TPHRV, and LF/HFHRV; [CS]: VLFBPV, VLFHRV, LFHRV, HFBPV, and LF/HFHRV) and also between Sham/PSD and SAD/CON ([PreCS]: VLFBPV, VLFHRV, LFBPV, LFHRV, HFBPV, HFHRV, TPBPV, TPHRV, and LF/HFHRV; [CS]: LFBPV, LFHRV, HFBPV, HFHRV, TPHRV, and LF/HFHRV). These results indicate that in both PreCS and CS trials, PSD could enhance the vasculomyogenic oscillations (VLFBPV) as the activation of myogenic vascular function, the sympathetic oscillations (LFBPV) as the activation of sympathetic outflows, and the thoracic hemodynamic oscillations (HFBPV) as the activation of the cardiopulmonary function. In contrast, except for LFBPV in the PreCS trial and LFHRV in the CS trial, SAD could attenuate the effects, as mentioned earlier of PSD in both PreCS and CS trials.

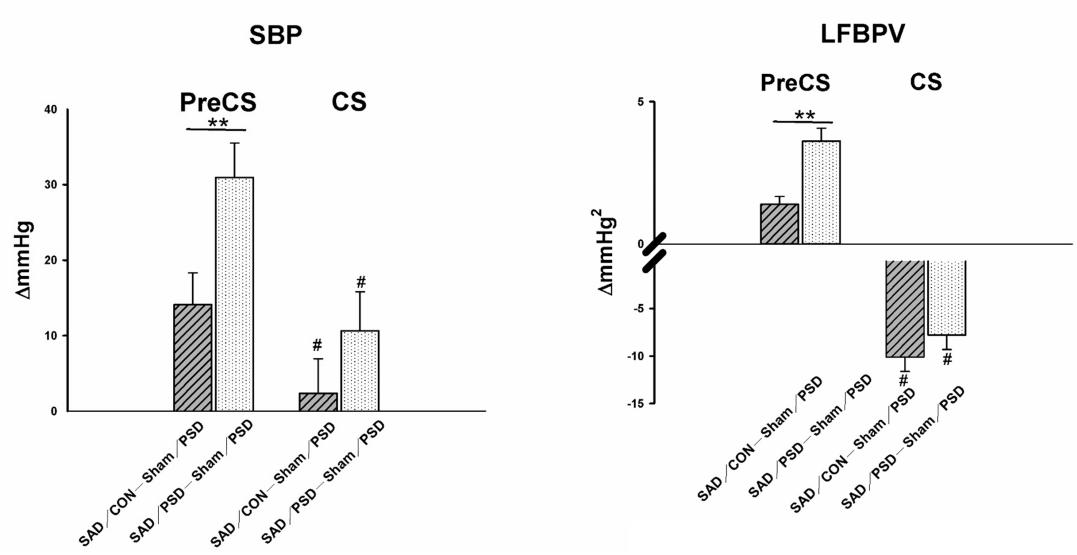


**Fig. 4. Data of value different in SBP level (A) and LFBPV power intensity (B) between two group rats in PreCS trial or CS trial.** The value of SAD/CON group rats minus the value of Sham/PSD group rats (stippled bars) and the value of SAD/PSD group rats minus the value of Sham/PSD (hatched bars). Data are presented as mean ± standard error (SEM). Differences were assessed by two-way ANOVA followed by *post hoc* Tukey method or Planned comparisons with paired Student's *t*-test and are indicated as follows: differences between group rats (**$p < 0.01$) and differences between the same parameter for CS versus PreCS (#$p < 0.05$) Abbreviations: CS, cold stress; PreCS, before CS; SBP, systolic blood pressure; LFBPV, the low frequency for blood pressure variability; Δ, difference.

Multiple-way ANOVA also revealed a significant main effect of within-subjects factor "trial" (**Supplementary Table 3**) driven by the differences between PreCS and CS in four groups: Sham/CON (VLFBPV, VLFHRV, LFBPV, LFHRV, HFBPV, TPBPV, and TPHRV), Sham/PSD (VLFBPV, VLFHRV, LFBPV, LFHRV, HFBPV, HFHRV, TPBPV, TPHRV, and LF/HFHRV), SAD/CON (VLFBPV, LFBPV, and HFBPV), and SAD/PSD (VLFBPV, LFBPV, LFHRV, and TPBPV). For the intensity difference between PreCS and CS of different frequencies (Table 1 and **Supplementary Table 4**), two-way ANOVA revealed significant main effects of SAD (VLFHRV, LFBPV, LFHRV, HFBPV, and HFHRV) and significant main effects of PSD (LFBPV, LFHRV, and HFBPV), which were driven by the differences between two groups: Sham/CON and Sham/PSD (LFBPV, LFHRV, and HFHRV), Sham/CON and SAD/CON (VLFHRV and HFBPV), Sham/PSD and SAD/PSD (VLFHRV, LFBPV, LFHRV, HFBPV, and HFHRV), and SAD/CON and SAD/PSD (VLFBPV). Further analysis by planned comparisons revealed a significant difference between Sham/CON and SAD/PSD (VLFHRV, LFBPV, and HFBPV) and between Sham/PSD and SAD/CON (VLFHRV, LFBPV, LFHRV, HFBPV, and HFHRV). These results show that all groups exert likewise inversed correlations between BPV and HRV intensities of those three dominant frequencies by CS (i.e., when compared CS with the respective PreCS, all three frequencies in CS generally show BPV intensity increases, but HRV intensity decreases). Furthermore, when comparing the height of spectral density of LFBPV and HFBPV, both SAD groups (SAD/CON and SAD/PSD) generally attenuated those two frequency intensities of the PSD-only groups (Sham/PSD) in the CS trial.

An inversed relationship between the magnitude of SBP level and the intensity of LFBPV power density of SAD/PSD and SAD/CON rats in CS is shown in Fig. 4. Compared with the Sham/PSD rats in PreCS, SBP and LFBPV power of both SAD/CON and SAD/PSD are higher than those of the Sham/PSD rats. However, in CS, SBP of SAD/CON and SAD/PSD rats are still higher, but their LFBPV power is much lower than that of the Sham/PSD rats and generally equipotent the Sham/CON rats.

### *3.3 Effects of PSD and SAD on coherence strength throughout the experiment*

The peak coherence values ($K^2_{IBI/SBP}$) for three dominant frequencies of four group rats are summarized in Fig. 5. When compared with Sham/CON in both PreCS and CS trials, Sham/PSD generally enlarges $K^2_{IBI/SBP}$ in LF region (Sham/PSD versus Sham/CON: 0.59 ± 0.02 versus 0.55 ± 0.03 [PreCS] and 0.61 ± 0.03 versus 0.57 ± 0.03 [CS] but decreases $K^2_{IBI/SBP}$ in HF region (Sham/PSD versus Sham/CON: 0.58 ± 0.01 versus 0.75 ± 0.03 [PreCS] and 0.52 ± 0.03 versus 0.76 ± 0.03 [CS]). Furthermore, SAD/CON and SAD/PSD attenuate the larger $K^2_{IBI/SBP}$ (> 0.58) of both Sham/CON and Sham/PSD in LF region (SAD/CON: 0.46 ± 0.03 [PreCS] and 0.42 ± 0.04 [CS]; SAD/PSD: 0.49 ± 0.03 [PreCS] and 0.52 ± 0.03 [CS]). The smaller and detached coherence ($K^2_{IBI/SBP} < 0.58$) of

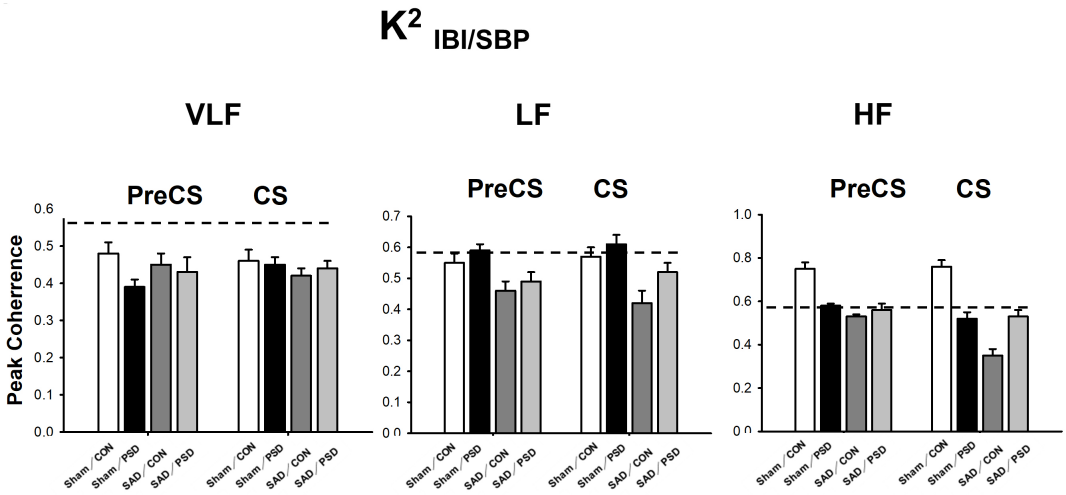


**Fig. 5. The relationship between systolic blood pressure and inter-beat interval oscillations in frequency regions as assessed by $K^2_{IBI/SBP}$ of different group rats throughout the experiment.** VLF, very-low-frequency; LF, low frequency; HF, high frequency; CS, cold stress; PreCS, before CS; $K^2_{IBI/SBP}$, peak coherence value; IBI, minter-beat interval.

Sham/PSD in HF region is still seen of SAD/CON and also of SAD/PSD (SAD/CON: 0.53 ± 0.01 [PreCS] and 0.35 ± 0.03 [CS]; SAD/PSD: 0.56 ± 0.03 [PreCS] and 0.53 ± 0.03 [CS]). Nevertheless, the smaller $K^2_{IBI/SBP}$ (<0.58) of all group rats in VLF region is seen throughout the experiment, which suggests their myogenic oscillations are detached.

## 4. Discussion

We investigated baroreflex function and spectral density changes by sinoaortic denervation. The study has enhanced our understanding of autonomic regulation of cardiovascular function in PSD and aversive CS. Here we discuss the SAD surgery first. As per the effects of SAD surgery (SAD/CON) compared with Sham surgery (Sham/CON) in the natural baseline condition, PreCS, we observed that SAD/CON rats, aligning with the previous studies in SAD animals [28–31], generally characterized of a decrease of TPHRV but sympathoexcitation, increases of SBP, HR, LFBPV, TPBPV and also LF/HFHRV ratio, these data indicate a sympathetic predominance of cardiac autonomic imbalance. We also observed a drastic VLFHRV reduction of the SAD/CON rats in this PreCS condition. We suspect the reduction of VLFHRV might result from the nitric oxide production because of shear stress by sympathoexcitation on resistance vasculature. The released nitric oxide might circulate into the adjacent myocardium to exert its depressive effects. Taken together of our observations, it supports the buffering action of baroreflex and its essential role in favoring BP stability. In addition, our findings further substantiate previous reports in the literature that SAD surgery alters particular frequency intensities of BPV and HRV and reverses baroreflex effects on specific autonomic outflows for cardiovascular homeostasis.

Previous studies indicate SAD animals are more sensitive to aversive threats than control animals [1,22–25]. When they are faced with stress, the SAD animal generally presented pressor, tachycardia, sympathoexcitation, and regional vasoconstriction responses were enhanced, suggesting baroreflex is beneficial for counteracting the enhancement of stress-elicited autonomic and hemodynamic perturbations. In this aspect, we further investigated the SAD rats in the aversive condition, CS. Compared with Sham/CON rats in CS, we observed that SAD/CON rats are generally characterized by a significant increase of SBP, LFHRV, and LF/HFHRV ratio, but HFBPV and HFHRV were substantially reduced. Based on these observations, we conclude that the net response of hemodynamic perturbations under CS is due to an interaction between autonomic cardiovascular regulation and baroreflex buffering effects. The reduction of HFBPV and HFHRV indicates a weakened baroreflex function of SAD/CON rats in the stressful CS, which concurs well with the previous reports [15,32] that SAD could trigger the cardiopulmonary effect on respiratory rate to attenuate the respiratory frequency.

Hereafter, we discuss the effects on autonomous cardiovascular regulation between PSD under sham surgery (Sham/PSD) and SAD surgery (SAD/PSD) group rats. As per the effects of hemodynamic perturbations of Sham/PSD rats with and without the CS impact, the results are consistent with our previous findings [12] that PSD could surge autonomic outflows to corresponding sympathetic activation (LFBPV and LFHRV increases) and parasympathetic activation (HFHRV increase) accompanied by a tendency to increase myogenic vascular oscillation (VLFBPV increases). Because of a high HFBP in both PreCS and CS conditions, our present findings support that Sham/PSD could influence cardiopulmonary function with higher thoracic activity. Nonetheless, the Sham/PSD rats further challenged by CS showed augmented LFBPV power, which in-

dicates PSD under CS has pushed vascular resistance to the critical limits, leading to the high SBP and profound hemodynamic perturbations.

It has been suggested that PSD could enhance the sympathetic drive to the kidney [33]. In addition, SAD and severe high-renin hypertension rats exhibit intensive BP changes similarly to control rats in natural sleep phases [26]. These findings indicate that overacting the renin-angiotensin system alters the central integration of baroreflex in natural sleep. Therefore, in the following studies, we focused on elucidating the impact of SAD (SAD/CON) on PSD (SAD/PSD) before and under CS. We observed, compared with Sham/CON and Sham/PSD rats, both SAD/CON and SAD/PSD rats displayed different contrast patterns between PreCS and CS of LFBPV changes (see Fig. 3). In PreCS, SAD/CON and SAD/PSD rats present an ascending higher LFBPV than the Sham/CON and Sham/PSD rats. However, in CS, the LFBPV of SAD/CON and SAD/PSD rats is much lower than that of the Sham/PSD rats but generally equipotent as that of the Sham/CON rats.

Subsequently, we turn to discuss whether PreCS and the following aversive CS might affect the hemodynamic perturbations in SAD/PSD rats. Compared with the Sham/CON rats in PreCS and CS, we observed that both SAD/CON and SAD/PSD rats generally showed similar trends in frequency power changes, except for the VLF-BPV and LHHRV intensities those of the SAD/PSD rats were much higher than those of the other group rats. On the other hand, compared with Sham/PSD rats in PreCS, we observed that SBP, HR, and LFBPV of SAD/CON and SAD/PSD rats were all higher than those of the Sham/PSD rats. However, in CS, the SBP and HR of both SAD/CON and SAD/PSD rats were still higher, but their LFBPV intensity was much lower than that of the Sham/PSD rats but roughly equal to that of the Sham/CON rats. This finding is impressive and beyond our expectations, i.e., an inversed relationship between SBP level and LFBPV intensity changes of the SAD/PSD rats in CS (see Fig. 4), which is against the loss of the baroreflex buffering effect we expected to observe. We discuss the possible mechanisms for this result below.

We speculate that pressor and tachycardia responses of SAD/PSD rats under CS are due to the synergic actions of several CS-elicited factors, for instance, adrenergic receptors, nitric oxide, sensory nerves, and non-neural pathways [7,10,11,34,35], which all might produce vasoconstriction, thereby increase SBP. Furthermore, baroreflex failure of SAD unmasks sympathetic inhibition on the heart, thereby increasing HR. Interestingly, in CS, higher SBP and HR levels of the SAD/PSD rats but strikingly much lower LF-BPV intensity than that of the Sham/PSD group rats. We ascribe this is because of the progressive inhibitory renorenal reflex effects. As mentioned previously, emerging findings revealed an interaction between ERSNA and ARNA. ERSNA regulates ARNA through norepinephrine released from sympathetic terminals, ERSNA increases, ARNA increases; in turn, the rise of ARNA will reduce ERSNA by initiating the inhibitory renorenal reflex [4,20,21]. In this perspective, we speculate that the decrease of LFBPV intensity of PSD/SAD rats is due to excessive activation of ERSNA by acute SAD under stressful CS, which increases renal vascular resistance to increase ARNA. The rise of ARNA activates inhibitory renorenal reflex; corresponding sympathetic outflows (LFBPV) therefore diminishes.

On the other hand, as per the coherence strength, we observed that both SAD/CON and SAD/PSD rats dissociated between BPV and HRV linkage ($K^2_{IBI/SBP} < 0.58$) at all three frequency regions. This phenomenon indicates baroreflex mechanism is essential for the linear relation between SBP and HR oscillations.

## 5. Conclusions

In conclusion, compared with the PSD-only rats, our present studies showed that the rats concurrently received SAD and PSD displayed prominent pressor and tachycardia responses throughout the experiment course but reduced the efferent sympathetic activities (LFBPV intensity) only in CS. We consider that reducing LFBPV intensity under CS is possible because of the activation of inhibitory renorenal reflex.

## Abbreviations

PSD, paradoxical sleep deprivation; SAD, sinoaortic denervation; CON, control; Sham/CON, control sham surgery group; SAD/CON, SAD surgery group; Sham/PSD, PSD under sham surgery group; SAD/PSD, PSD under SAD group; ARNA, afferent renal nerve activity; ERSNA, efferent renal sympathetic nerve activity; CS, cold stress; PreCS, the baseline trial before CS; BP, blood pressure; SBP, systolic blood pressure; HR, heart rate; BPV, blood pressure variability; HRV, heart rate variability; VLF, very-low-frequency; LF, low frequency; HF, high frequency; LF/HFHRV, the LF/HF ratio of HRV; $K^2_{IBI/SBP}$, coherence value; IBI, inter-beat interval.

## Author contributions

CST and SHT contributed equally to this work, supervised the project and were responsible for interpreting and writing the manuscript. YPL contributed to the conception and design of the study. CCL and YCL assisted in data analysis provided technical expertise and data interpretation. All authors approved the final version of the manuscript for publication.

## Ethics approval and consent to participate

The study design according to a protocol is approved by the National Defense Medical Center (NDMC) animal care committee (IACUC-13-170). Experiments were car-

ried out following the guidelines laid down by the animal ethics/welfare committee and conform to the principles and regulations of this Journal.


## Acknowledgment

The authors would like to thank Chan-Fan Young and Huei-Yin Siao for their technical assistance.

## Funding

This research was funded by the Ministry of Science and Technology and and the CHGH-NDMC cooperative research project, Taiwan, R.O.C, grant number, MOST 103-2320-B-350-001, MOST 108-2314-B-016-047-MY3, CHNDMC-110-6.


## Conflict of interest

The authors declare no conflict of interest. CST is serving as one of the Editorial Board members of this journal. We declare that CST had no involvement in the peer review of this article and has no access to information regarding its peer review. Full responsibility for the editorial process for this article was delegated to LDG.

## Supplementary material

Supplementary material associated with this article can be found, in the online version, at https://doi.org/10.31083/j.jin2103075.

## References


[1] Biaggioni I, Shibao CA, Diedrich A, Muldowney JAS, Laffer CL, Jordan J. Blood Pressure Management in Afferent Baroreflex Failure. Journal of the American College of Cardiology. 2019; 74: 2939–2947.

[2] Parati, Di Rienzo M, Omboni, Ulian, Mancia. Blood pressure variability over 24 hours: its different components and its relationship to the arterial baroreflex. Journal of Sleep Research. 1995; 4: 21–29.

[3] Gelman S, Mushlin P, Weiskopf R. Catecholamine-induced Changes in the Splanchnic Circulation Affecting Systemic Hemodynamics. Anesthesiology. 2004; 100: 434–439.

[4] Kopp UC. Role of renal sensory nerves in physiological and pathophysiological conditions. American Journal of Physiology-Regulatory, Integrative and Comparative Physiology. 2015; 308: R79–R95.

[5] Mai TH, Garland EM, Diedrich A, Robertson D. Hepatic and renal mechanisms underlying the osmopressor response. Autonomic Neuroscience. 2017; 203: 58–66.

[6] Linz D, Hohl M, Elliott AD, Lau DH, Mahfoud F, Esler MD, *et al*. Modulation of renal sympathetic innervation: recent insights beyond blood pressure control. Clinical Autonomic Research. 2018; 28: 375–384.

[7] Tung C, Tsai S, Lin J, Lin Y, Liu Y. Portal vein innervation underlying the pressor effect of water ingestion with and without cold stress. Chinese Journal of Physiology. 2020; 63: 53–59.

[8] Salman IM. Major Autonomic Neuroregulatory Pathways Underlying Short- and Long-Term Control of Cardiovascular Function. Current Hypertension Reports. 2016; 18: 18.

[9] Berthoud H, Neuhuber WL. Functional and chemical anatomy of the afferent vagal system. Autonomic Neuroscience. 2000; 85: 1–17.

[10] Lin YH, Liu YP, Lin YC, Lee PL, Tung CS. Characterization of the role of endogenous nitric oxide in myogenic vascular oscillations during cooling-evoked hemodynamic perturbations of rats. Canadian Journal of Physiology and Pharmacology. 2017; 95: 803–810.

[11] Lin YH, Liu YP, Lin YC, Lee PL, Tung CS. Cooling-evoked hemodynamic perturbations facilitate sympathetic activity with subsequent myogenic vascular oscillations via alpha2-adrenergic receptors. Physiological Research. 2018; 66: 449–457.

[12] Yang YN, Liu YP, Hsieh MT, Lin YC, Tung CS. Effects of prolonged paradoxical sleep deprivation with or without acute cold stress on hemodynamic perturbations in rats. Stress. 2018; 21: 520–527.

[13] Baselli G, Cerutti S, Civardi S, Liberati D, Lombardi F, Malliani A, *et al*. Spectral and cross-spectral analysis of heart rate and arterial blood pressure variability signals. Computers and Biomedical Research. 1986; 19: 520–534.

[14] Cohen MA, Taylor JA. Short-term cardiovascular oscillations in man: measuring and modelling the physiologies. The Journal of Physiology. 2002; 542: 669–683.

[15] Di Rienzo M, Parati G, Radaelli A, Castiglioni P. Baroreflex contribution to blood pressure and heart rate oscillations: time scales, time-variant characteristics and nonlinearities. Philosophical Transactions of the Royal Society a: Mathematical, Physical and Engineering Sciences. 2009; 367: 1301–1318.

[16] Irigoyen MC, Moreira ED, Ida F, Pires M, Cestari IA, Krieger EM. Changes of renal sympathetic activity in acute and chronic conscious sinoaortic denervated rats. Hypertension. 1995; 26: 1111–1116.

[17] Sei H, Morita Y, Tsunooka K, Morita H. Sino-aortic denervation augments the increase in blood pressure seen during paradoxical sleep in the rat. Journal of Sleep Research. 1999; 8: 45–50.

[18] Piratello AC, Moraes-Silva I, Paulini J, Souza PR, Sirvente R, Salemi V, *et al*. Renin angiotensin system and cardiac hypertrophy after sinoaortic denervation in rats. Clinics. 2010; 65: 1345–1350.

[19] Rodrigues FL, de Oliveira M, Salgado HC, Fazan R. Effect of baroreceptor denervation on the autonomic control of arterial pressure in conscious mice. Experimental Physiology. 2011; 96: 853–862.

[20] Jackson EK. Autonomic Control of the Kidney. In D. Robertson, I Biaggioni, G. Burnstock, P.A. Low, & F.R. Paton (eds.), Primer on the Autonomic Nervous System (pp. 215–220). Academic Press: Oxford. 2012.

[21] Johns EJ. The neural regulation of the kidney in hypertension and renal failure. Experimental Physiology. 2014; 99: 289–294.

[22] Buchholz RA, Hubbard JW, Keeton TK, Nathan MA. Cardiovascular and neuroendocrine responses to behavioral stress after central or peripheral barodenervation in rats. Brain Research. 1986; 365: 360–364.

[23] Nakata T, Berard W, Kogosov E, Alexander N. Effect of environmental stress on release of norepinephrine in posterior nucleus of the hypothalamus in awake rats: role of sinoaortic nerves. Life Sciences. 1991; 48: 2021–2026.

[24] Zhang ZQ, Julien C, Barrès C. Baroreceptor modulation of regional haemodynamic responses to acute stress in rat. Journal of the Autonomic Nervous System. 1996; 60: 23–30.

[25] Dos Reis DG, Fortaleza EAT, Tavares RF, Corrêa FMA. Role of the autonomic nervous system and baroreflex in stress-evoked cardiovascular responses in rats. Stress. 2014; 17: 362–372.

[26] Silveira NP, Moreira ED, Drager LF, Silva GJJ, Krieger EM. Effects of sinoaortic denervation on hemodynamic parameters during natural sleep in rats. Sleep. 2008; 31: 328–333.

[27] deBoer RW, Karemaker JM, Strackee J. Hemodynamic fluctua-

tions and baroreflex sensitivity in humans: a beat-to-beat model. the American Journal of Physiology. 1987; 253: H680–H689.
[28] Alexander N, Velasquez MT, Decuir M, Maronde RF. Indices of sympathetic activity in the sinoaortic-denervated hypertensive rat. The American Journal of Physiology. 1980; 238: H521–H526.
[29] Saavedra JM, Krieger EM. Early increase in adrenomedullary catecholamine synthesis in sinoaortic denervated rats. Journal of the Autonomic Nervous System. 1987; 18: 181–183.
[30] Mancia G, Parati G, Castiglioni P, di Rienzo M. Effect of sinoaortic denervation on frequency-domain estimates of baroreflex sensitivity in conscious cats. The American Journal of Physiology. 1999; 276: H1987–H1993.
[31] Radaelli A, Mancia G, De Carlini C, Soriano F, Castiglioni P. Patterns of cardiovascular variability after long-term sinoaortic denervation in unanesthetized adult rats. Scientific Reports. 2019; 9: 1232.
[32] Amorim MR, Bonagamba LGH, Souza GMPR, Moraes DJA, Machado BH. Role of respiratory changes in the modulation of arterial pressure in rats submitted to sino-aortic denervation. Experimental Physiology. 2017; 101: 1359–1370.
[33] Perry JC, Bergamaschi CT, Campos RR, Andersen ML, Montano N, Casarini DE, *et al*. Sympathetic and angiotensinergic responses mediated by paradoxical sleep loss in rats. Journal of the Renin-Angiotensin-Aldosterone System. 2011; 12: 146–152.
[34] Kellogg DL. In vivo mechanisms of cutaneous vasodilation and vasoconstriction in humans during thermoregulatory challenges. Journal of Applied Physiology. 2006; 100: 1709–1718.
[35] Alba BK, Castellani JW, Charkoudian N. Cold-induced cutaneous vasoconstriction in humans: Function, dysfunction and the distinctly counterproductive. Experimental Physiology. 2019; 104: 1202–1214.